Dripping-Jetting Transitions in a Dripping Faucet

Bala Ambravaneswaran, Hariprasad J. Subramani, Scott D. Phillips, and Osman A. Basaran*

School of Chemical Engineering, Purdue University, West Lafayette, Indiana 47907, USA
(Received 20 December 2003; published 15 July 2004)

Fascinating dynamics is known to result when the flow rate Q at which water drips from a faucet varies. Starting with simple (period-1) dripping, the system transitions as Q increases to complex dripping, where it exhibits period-n ($n = 2, 4, \ldots$) and chaotic responses, and then jets once Q exceeds a threshold. New experiments and simulations show that high viscosity (μ) liquids, e.g., syrup, transition directly from simple dripping to jetting as Q increases. Phase diagrams showing transitions between simple and complex dripping and jetting in (Q, μ) space are developed. Values of Q for transition from dripping to jetting are estimated from scaling arguments and shown to accord well with simulations.

Water dripping from a leaky faucet [1], ink being squirted from an ink-jet nozzle [2], a DNA microarray being deposited on a biochip [3], and microencapsulation [4] are common examples of situations involving drop formation [5]. In each case, many drops in sequence are formed from a nozzle, about one drop per second in the case of the ordinary leaky faucet and thousands of drops per second in the case of the versatile ink-jet printer. Figure 1 shows schematically the evolution of the dynamics with increasing flow rate Q when a Newtonian liquid of viscosity μ such as water flows at a constant flow rate from a tube of radius R into air. For small Q, primary drops as well as much smaller satellites form periodically in time, as shown in Fig. 1(a) [6–8]. At a critical value of Q, satellites cease to form and simple, period-1 dripping ensues, where every drop is the same, as shown in Fig. 1(b). As Q is increased further, simple dripping gives way to complex dripping, where nonlinear dynamical phenomena such as period doubling, chaos, and hysteresis are observed [1,9]. For sufficiently large values of Q, dripping gives way to jetting, where drops detach from the ends of long columns of liquid far downstream of the tube exit, as shown in Fig. 1(c) [9,10]. The goals of this Letter are to answer the long-standing questions of how the faucet's response would change if a high viscosity liquid such as syrup were used in lieu of water and whether small changes in μ result in large changes in the faucet's response.

Since Shaw's [1] pioneering work inaugurating two decades of studies of leaky faucets, experiment, theory, and computation have been used to gain insights into dripping. Two sorts of experimental approach have been utilized to date. One of these has focused on measuring time intervals between drops, $t_1, t_2, \ldots, t_i, \ldots$, where t_i is the time interval between the ith and $(i-1)$th drops [1,9]. Time interval data are then examined through time return maps, where each point in the map is determined by the ordered pair (t_n, t_{n+1}) for some n, to make inferences about the system's nonlinear response [1,9,11,12]. The other experimental approach, which is typically used

along with drop counting, utilizes high-speed imaging to capture the dynamics of formation of many drops in sequence [9,12]. Complementing the early experimental works in the field, several workers have used simple theories based on spring-mass models to surmise the faucet's response [1,13,14]. Recently, researchers have started to use computational approaches to predict the formation of hundreds of drops in sequence. These [8,9] have relied on solving one-dimensional (1D), slender-jet approximations to the Navier-Stokes (NS) equations developed by Eggers and Dupont [15] or analogous 1D approximations [11,14]. As numerically solving the NS equations takes about 100 times longer than solving the 1D model equations, the former approach has not been used to date in computing the dynamics beyond the formation of a few drops [7,16,17].

Aside from exploring the range of nonlinear dynamical phenomena that occur for a particular liquid issuing from a given tube as Q is varied, several papers have addressed, albeit only partially, the equally important issue of identifying the conditions for transitions to occur between various flow regimes for liquids of widely
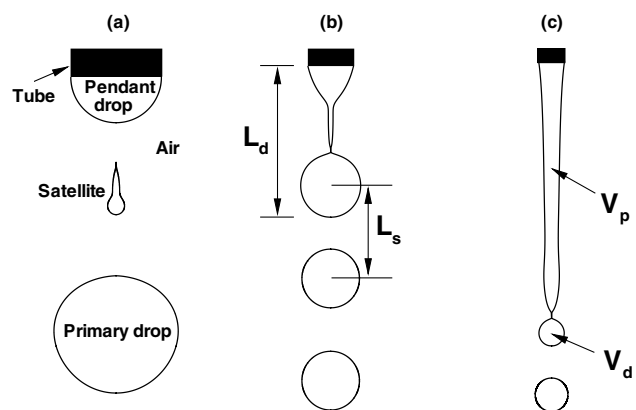
FIG. 1.   Regimes of drop formation. (a) Dripping with satellite formation, (b) dripping without satellite formation, and (c) jetting. The flow rate increases from left to right.

disparate properties. For example, Ambravaneswaran *et al.* [8] have determined the variation with viscosity of the critical value of Q, Q_c, beyond which satellites no longer form. Zhang [7] has determined Q_c in the limit of small μ. The transition from dripping to jetting has been studied for over a century, unfortunately before good understanding of nonlinear dynamics was available, when liquid drops form in air [18] as well as in another liquid [19]. Recently, Clanet and Lasheras [10] have developed an analytical expression for Q_c in the inviscid limit. Therefore, a major goal of this Letter is to develop phase diagrams that show transitions between simple and complex dripping and jetting in (Q, μ) space. Remarkably, a quantitative criterion for the onset of jetting is still lacking. Many authors use qualitative criteria to decide when a liquid is no longer dripping but jetting. For example, Clanet and Lasheras [10] employ the *ad hoc* convention that the liquid is jetting when $L_d \approx 20R$, where L_d is the limiting length or the drop length at breakup [cf. Fig. 1(b)]. Unfortunately, this criterion fails for high viscosity liquids, as their L_d can be of $\mathcal{O}(100R)$ or larger even when $Q \rightarrow 0$ [6,8]. Quantitative criteria to determine the onset of jetting are also developed in this Letter.

Here the dynamics of the leaky faucet is analyzed both computationally and experimentally. The computations rely on solving the 1D slender-jet equations for the shape of a drop of an incompressible Newtonian liquid forming out of a tube of outer radius R and negligible wall thickness and for the axial velocity within the drop

$$\frac{\partial v_z}{\partial t} = -v_z \frac{\partial v_z}{\partial z} - \frac{\partial(2\mathcal{H})}{\partial z} + 3\mathrm{Oh}\frac{1}{h^2}\frac{\partial}{\partial z}\left(h^2 \frac{\partial v_z}{\partial z}\right) + G, \tag{1}$$

$$\frac{\partial h}{\partial t} = -v_z \frac{\partial h}{\partial z} - \frac{1}{2}h\frac{\partial v_z}{\partial z}, \tag{2}$$

where t is the time, $h(z, t)$ is the drop radius at a distance z from the tube exit, $v_z(z, t)$ is the axial velocity, and $\mathcal{H}$ is the mean curvature. Equations (1) and (2) are already dimensionless, as length is measured in units of R and time is measured in units of $\sqrt{\rho R^3/\sigma}$, where ρ is the density and σ is the surface tension. Three dimensionless groups govern the dynamics. Two of these, the Ohnesorge number Oh and the Bond number G, appear in Eq. (1), and the third, the Weber number We, arises when a plug flow velocity profile is imposed at the tube exit in the 1D formulation [8]. These groups are defined as $\mathrm{Oh} \equiv \mu/\sqrt{\rho R\sigma}$, $G \equiv \rho R^2 g/\sigma$, where g is the gravitational acceleration, and $\mathrm{We} \equiv \rho U^2 R/\sigma$, where $U \equiv Q/\pi R^2$. Equations (1) and (2) are solved subject to the boundary conditions that (i) at $z = 0$, $h = 1$ and $v_z = \sqrt{\mathrm{We}}$, and (ii) at $z = L(t)$, where $L(t)$ is the instantaneous length of the drop, $h = 0$ and $v_z = dL/dt$. The initial condition is a static pendant hemispherical drop, viz., $h = \sqrt{1 - z^2}$ and

$v_z = 0$ for $0 \leq z \leq 1$. The system of Eqs. (1) and (2) is solved using the finite element method [8].

In the experiments, a liquid is driven at a constant flow rate through a tube by a Sage MP362 syringe pump. A high-speed Kodak Ektapro imager is employed to visualize the dynamics. Liquids used in the experiments include water, glycerol-water mixtures at various concentrations of glycerol, and silicone oils. By varying drop liquids, tube radii, and flow rates, the following ranges of the dimensionless groups have been accessed: $3 \times 10^{-3} \leq \mathrm{Oh} \leq 2$, $0.31 \leq G \leq 0.97$, and $0 \leq \mathrm{We} \leq \mathcal{O}(1)$.

Two gross flow transitions that arise as We is increased are of interest here. The first, which signals the transition from simple dripping [cf. Fig. 1(a)] to complex dripping and occurs when $\mathrm{We} = \mathrm{We}_d$, can be detected as explained earlier. The second, which signals the transition from dripping to jetting and occurs when $\mathrm{We} = \mathrm{We}_j$, turns out to be easily detectable because certain measures of the dynamics, as shown in Fig. 2, undergo sudden and large changes at the same time that the observed dynamics transitions to that depicted in Fig. 1(c). As shown in Fig. 2, the measures that undergo sudden and large increases (decreases) are (a) the dimensionless limiting length L_d/R; (b) the ratio of the distance L_s between the centers of mass of the drop that is about to form and the previously formed drop [cf. Fig. 1(b)] and L_d, viz. L_s/L_d; and (c) the ratio of the volume of the drop that is about to form, V_d, to that of the drop that is pendant from the tube, V_p, viz. V_d/V_p [cf. Fig. 1(c)].
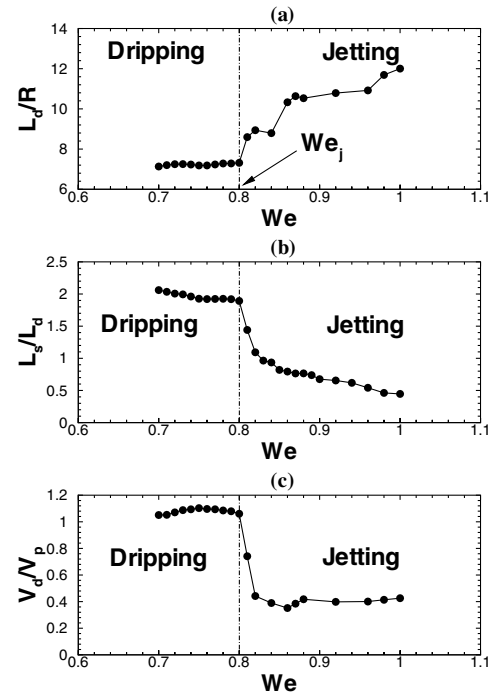
FIG. 2. Computed variation with We of three quantitative measures of the dynamics for detecting transition from dripping to jetting. Here $\mathrm{Oh} = 0.01$ and $G = 0.5$.

Figure 3 depicts a phase or an operability diagram in (We, Oh) space, i.e., dimensionless (Q, μ) space, that shows computationally and experimentally obtained curves that identify locations in the parameter space where the dynamics transitions from one regime to another. Given a liquid with properties ρ, μ, and σ, and a tube of radius R, which then determine Oh and G, the flow rate (We) is slowly increased from zero [9]. As We increases, the system may transition from simple to complex dripping when We = We_d, which for each liquid-tube pair then identifies a point $(\mathrm{We}_d(\mathrm{Oh}, G), \mathrm{Oh})$ on a curve marked as We_d in Fig. 3 that separates the region of the parameter space where simple dripping occurs from that where complex dripping occurs. Thereafter, as We is increased, the system may eventually transition from dripping to jetting when We = We_j, which then identifies a point $(\mathrm{We}_j(\mathrm{Oh}, G), \mathrm{Oh})$ on a curve marked as We_j in Fig. 3 that separates the region of the parameter space where jetting occurs from that where dripping occurs. Figure 3 shows that computed and experimental results accord well when Oh $\gtrsim 0.1$ and that the computed We_d curve agrees well with the experimental one for Oh as small as 0.02. That the computed We_j curve is not quantitatively accurate for small values of Oh accords with Ref. [8], where it is shown that the 1D model becomes less accurate for low Oh liquids as We increases. Computed results are not shown for Oh < 0.02, as solutions of NS equations and experiments with low Oh drops [8,16,17] show that drop shapes are overturned before pinch-off and the effects of the reverse flow emanating from the pinching necks of drops are felt within the tube, neither of which can be accounted for by 1D models.

Since a change in viscosity is typically accompanied by a change in surface tension and density and because the radii of tubes available to us cannot be varied continuously, in Fig. 3 G, which ideally should be held constant while Oh is varied, varies modestly by a factor of 3 while Oh varies by a factor of 1000. Figure 4 shows a computed phase diagram in (We, Oh) space where $G = 0.5$. Figure 4 and also Fig. 3 show that when Oh exceeds a critical value Oh_c, a leaky faucet transitions directly from simple dripping to jetting when We $\geq \mathrm{We}_j$. Thus, high viscosity liquids do not exhibit complex dripping in contrast to their low viscosity counterparts.

Figure 4 shows that when $G = 0.5$, a leaky faucet exhibits complex dripping when Oh = 0.1 for $\mathrm{We}_d \approx 0.12 < \mathrm{We} < \mathrm{We}_j \approx 0.26$. A detailed study of the faucet for this set of parameters is reported in Ref. [9], where it is shown that the system exhibits period-2, period-4, period-1, and hysteretic responses as We is varied. Figure 4 shows that Oh, or equivalently μ holding everything else constant, must be increased by more than a factor of 5 for the system not to exhibit complex dripping. Moreover, Ambravaneswaran *et al.* [9] and Yildirim and Basaran [20] have shown that Oh, or μ, must be decreased by roughly the same amount for the system to exhibit chaotic dripping.

Figure 5 shows computed snapshots of the dynamics when $G = 0.5$ at two Oh values. In Figs. 5(a) and 5(b), Oh = 0.01 and the transition from dripping to jetting at this value of Oh occurs when We = $\mathrm{We}_j = 0.8$. For the cases shown in Figs. 5(c) and 5(d), Oh = 0.5, which is the Ohnesorge number at which the triple point in Fig. 4
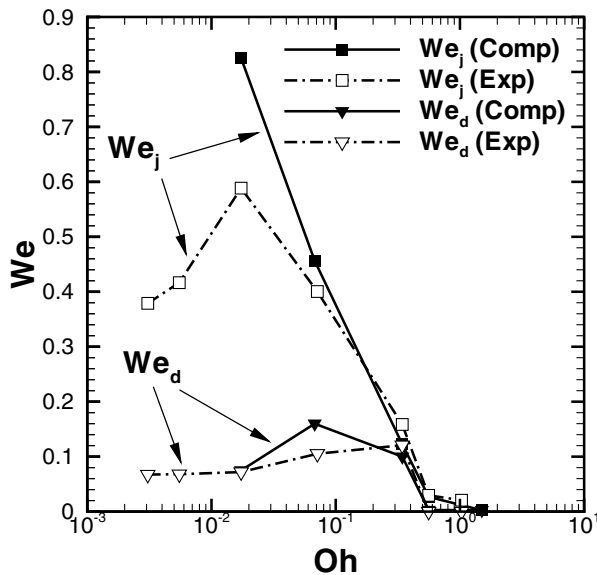
FIG. 3. Phase diagram that shows computationally and experimentally obtained curves, indicated by (Comp) and (Exp), respectively, that identify the values of We where the dynamics transitions from simple to complex dripping, We_d, and from dripping to jetting, We_j. Here $0.31 \leq G \leq 0.97$.
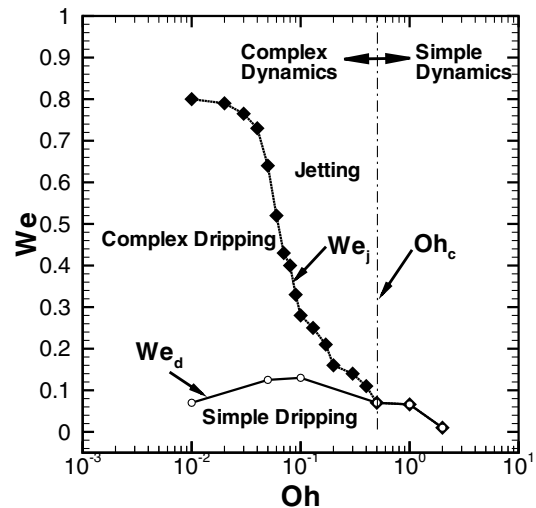
FIG. 4. A computed phase diagram in (We, Oh) space when $G = 0.5$. The curves We_d and We_j have the same meanings as in Fig. 3. When Oh > Oh_c, the leaky faucet transitions directly from simple dripping to jetting.
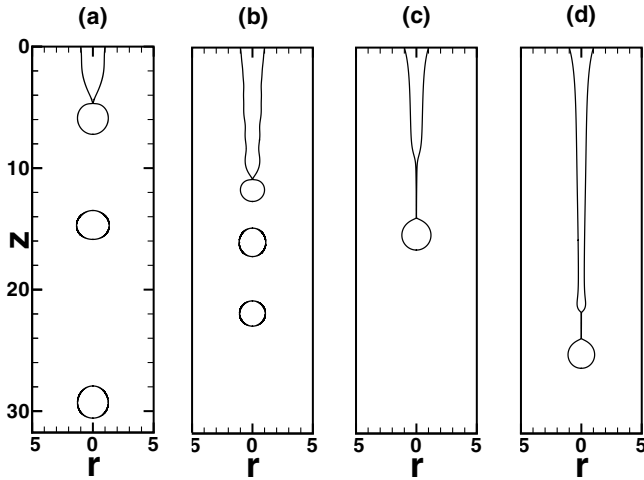
FIG. 5.   Computed snapshots of the dynamics when $G = 0.5$. (a) $Oh = 0.01$ and $We = 0.73$, dripping; (b) $Oh = 0.01$ and $We = 0.98$, jetting; (c) $Oh = 0.5$ and $We = 0.07$, dripping; and (d) $Oh = 0.5$ and $We = 0.071$, jetting.

occurs and where the system transitions directly from dripping to jetting when $We = We_j = 0.0705$.

A physical understanding of how the critical Weber number for transition from dripping to jetting We_j varies with the Ohnesorge number Oh (cf. Fig. 4) can be developed by comparing the relevant characteristic time scales of the dynamics. Previous studies of pinch-off of fluid interfaces have shown that the relevant time scale for capillary breakup depends on the value of the Ohnesorge number [21]. Thus, the time scale for capillary breakup scales as $t_c \equiv \sqrt{\rho R^3/\sigma}$ when $Oh \ll 1$, $t_\nu \equiv \mu R/\sigma$ when $Oh \gg 1$, and $t_\mu \equiv \mu^3/(\rho\sigma^2)$ when $Oh \sim 1$ [21]. In all cases, the time scale for the flow t_f scales as R/U. It is reasonable to expect that the transition to jetting should occur when the flow beats out one or another of the three time scales for capillary breakup. Thus, when $Oh \ll 1$, $t_f < t_c$ and hence $We > c_I$, where c_I is an $\mathcal{O}(1)$ constant, for jetting to occur. On the other hand, when $Oh \gg 1$, $t_f < t_\nu$ and hence $Ca = Oh\sqrt{We} > c_V$, where $Ca = \mu U/\sigma$ is the capillary number and c_V is another $\mathcal{O}(1)$ constant, for jetting to occur. However, when $Oh \sim 1$, $t_f < t_\mu$ and hence $CaOh^2 = Oh^3\sqrt{We} > c_{IV}$, where c_{IV} is yet another $\mathcal{O}(1)$ constant, for jetting to occur. Figure 4 shows that at low Oh, jetting occurs when We_j is $\mathcal{O}(1)$, in accord with this simple theory. Figure 4 also shows that at high Oh, We_j decreases as Oh increases, also in accord with the theory, and computed results show that $We_j \sim Oh^{-2}$. Figure 4 further shows that at intermediate Oh, We_j falls sharply as Oh rises, once again in agreement with the theory, and computed results show that $We_j \sim Oh^{-6}$.

Tube wall thickness [6] or outlet type [12] are important parameters for which 1D models cannot account. Experiments have also been carried out to study the effect of the ratio of the inner tube radius to the outer radius T_r on We_d and We_j using water. It has been found that varying T_r does not significantly affect We_d but a small decrease in T_r results in an appreciable increase in We_j.

According to the foregoing results, while low-viscosity liquids such as water may exhibit complex nonlinear dynamical responses, replacing water by high-viscosity liquids may eliminate all the interesting responses that a leaky faucet may exhibit. While increasing μ can make the faucet's response less nonlinear, certain effects such as non-Newtonian rheology [22] and electric fields [23] are likely to increase the complexity of its response because they introduce new nonlinearities. The results of a study examining the effects of shear thinning and extensional thickening will be reported shortly [20].

*Electronic address: obasaran@ecn.purdue.edu
[1] R. Shaw, *The Dripping Faucet as a Model Chaotic System* (Aerial Press, Santa Cruz, CA, 1984).
[2] H. P. Le, J. Imaging Sci. Technol. **42**, 49 (1998).
[3] R. F. Service, Science **282**, 396 (1998).
[4] A. M. Gañán-Calvo, Phys. Rev. Lett. **80**, 285 (1998).
[5] O. A. Basaran, AIChE J. **48**, 1842 (2002).
[6] X. Zhang and O. A. Basaran, Phys. Fluids **7**, 1184 (1995).
[7] X. Zhang, J. Colloid Interface Sci. **212**, 107 (1999).
[8] B. Ambravaneswaran, E. D. Wilkes, and O. A. Basaran, Phys. Fluids **14**, 2606 (2002).
[9] B. Ambravaneswaran, S. D. Phillips, and O. A. Basaran, Phys. Rev. Lett. **85**, 5332 (2000).
[10] C. Clanet and J. C. Lasheras, J. Fluid Mech. **383**, 307 (1999).
[11] P. Coullet, L. Mahadevan, and C. Riera, Prog. Theor. Phys. Suppl. **139**, 507 (2000).
[12] A. D'Innocenzo, F. Paladini, and L. Renna, Phys. Rev. E **65**, 056208 (2002).
[13] A. D'Innocenzo and L. Renna, Int. J. Theor. Phys. **35**, 941 (1996).
[14] K. Kiyono and N. Fuchikami, J. Phys. Soc. Jpn. **68**, 3259 (1999).
[15] J. Eggers and T. F. Dupont, J. Fluid Mech. **262**, 205 (1994).
[16] E. D. Wilkes, S. D. Phillips, and O. A. Basaran, Phys. Fluids **11**, 3577 (1999).
[17] A. U. Chen, P. K. Notz, and O. A. Basaran, Phys. Rev. Lett. **88**, 174501 (2002).
[18] S. W. J. Smith and H. Moss, Proc. R. Soc. London, Ser. A **93**, 373 (1917).
[19] G. F. Scheele and B. J. Meister, AIChE J. **14**, 15 (1968).
[20] O. E. Yildirim and O. A. Basaran (to be published).
[21] J. R. Lister and H. A. Stone, Phys. Fluids **10**, 2758 (1998).
[22] J. Cooper-White, J. Fagan, V. Tirtaatmadja, D. Lester, and D. Boger, J. Non-Newtonian Fluid Mech. **106**, 29 (2002).
[23] M. Cloupeau and B. Prunet-Foch, J. Electrost. **25**, 165 (1990).